

Equivalent Circuit Models and Analysis of Electrochemical Impedance Spectra of Caffeine Solutions and Beverages

Gourav Bhattacharya¹, Ashish Mathur², Srikanta Pal³, James McLaughlin⁴ and Susanta Sinha Roy^{1,*}

¹Department of Physics, School of Natural Sciences, Shiv Nadar University, Gautam Budh Nagar 201314, Uttar Pradesh, India.

²Amity Institute of Nanotechnology, Amity University, Sector-125, Noida 201303, Uttar Pradesh, India.

³Department of Electrical Engineering, School of Engineering, Shiv Nadar University, Gautam Budh Nagar 201314, Uttar Pradesh, India.

⁴Nanotechnology and Integrated Bioengineering Centre, Jordanstown Campus, University of Ulster, Newtownabbey, BT37 0QB, Northern Ireland, United Kingdom.

*E-mail: susanta.roy@snu.edu.in

Received: 24 November 2015 / Accepted: 18 May 2016 / Published: 4 June 2016

In this study, a non-faradaic electrochemical impedance spectroscopy has been employed for estimation of caffeine concentration in beverages. Impedance spectra were recorded by using a two electrode system without adding any redox reagents in the measured solutions. Electrochemical impedance data of caffeine solutions in pure water and beverages were measured and an appropriate equivalent electrical circuit model is developed to help in this investigative analysis. The interaction of caffeine molecules with the electrodes was primarily correlated to the formation of electrical double-layer at modified interface. Overall system impedance ($|Z|$), inverse of solution resistance ($1/R_s$) and constant phase element of the system were further investigated from the equivalent electrical circuit and plotted as a function of pure caffeine concentration. Finally, the results obtained from spiked diluted cola beverages were compared with the pure caffeine sample.

Keywords: Caffeine, Impedance Spectroscopy, Circuit modeling

1. INTRODUCTION

Caffeine (1,3,7-trimethylxanthine) is one of the key ingredients in many drinks, such as tea, coffee, sodas and energetic drinks [1,2]. Caffeine influences the central nervous system [3], and is a natural psychoactive stimulant [4]. It is mainly extracted from a tree called *coffea arabica* and is also present in tea leaves, coffee seeds, cocoa beans, cola nuts etc. [5]. It is basically an alkaloid [6], and

has medicinal value, especially in medicines for pain relief [7]. Though caffeine is a popular stimulant, but the overdose of it, may result in various physical illnesses, such as, cardiovascular problems, mutation of human DNA, nausea, seizures [8,9,10,11]. It also leads to hyperactivity, kidney problems and many other life threatening diseases [12,13,14]. Therefore, it is very important to detect the amount of caffeine present in drinks to avert the potential negative effects.

In recent years, many techniques have been developed to detect caffeine from a mixture of caffeine containing beverages. The traditional detection processes are based on spectroscopic study [15]. A combined chromatography (gas, liquid) - mass spectroscopy (MS), UV-Vis, IR and NMR techniques are mostly used detection of caffeine [16,17,18]. Though these techniques have greater sensitivity, but they essentially require sophisticated and expensive instrumentation and simultaneously takes longer time for analysis as the detection is performed after multiple complex phases (e.g. sample derivation, extraction, purification etc.). Electrochemical method has emerged as another popular tool for the precise detection of various chemical and biological species. Differential Pulse Voltammetry (DPV) [19,20] and Cyclic Voltammetry (CV) [21,22] are the two major electrochemical detection methods. In recent years, electrochemical impedance Spectroscopy (EIS) has been extensively studied to detect biological and organic samples [23,24,25]. EIS is emerging as an important tool for modern sensors. It is rapid, label free and sensitive process which fits perfectly with the modern world's requirements. However, possible applications of EIS for the comparison of caffeine molecules in standard and real samples have not been studied yet.

Present work describes the use of EIS for the equivalent circuit modeling and the comparison of caffeine concentration in pure caffeine and cola beverages. The experimental system allows us to understand the electrochemical activity of caffeine on electrodes surface. Impedance data is also modeled using an appropriate equivalent electrical circuit and finally the obtained parameters from the equivalent circuit was also compared and analyzed.

2. EXPERIMENTAL

2.1. Materials

Anhydrous caffeine ($C_8H_{10}N_4O_2$) was purchased from QFC Fine Chem (India) and used without any further purification. All aqueous solutions were prepared by using ultrapure water by Millipore-Q systems (Merck, USA) where the measured electrical resistance of water was around 18 M Ω at room temperature (298 K). Three different cola beverages were bought from a local store.

2.2 Electrochemical impedance spectroscopy

Impedance spectroscopy data was obtained from Autolab Potentiostat Galvanostat PGSTAT302N (METRHOM AUTOLAB B.V Netherlands). All the measurements were carried out in FRA potential scan mode with a two electrode set up. A platinum disk of 2mm diameter was used as the working electrode), whereas a platinum wire of 40 mm length was used as the counter electrode

[26]. These electrodes were kept in the solution at a distance of 18 mm apart throughout the experiment. Caffeine solutions with different concentrations (100 mM to $\sim 450 \mu\text{M}$) were prepared utilizing Millipore ultrapure water by ultrasonication. The cola beverages (CB1, CB2 and CB3) were diluted 10 and 15 folds and then mixed with known concentration of caffeine solution. All the measurements were carried out using 30 ml of solution (15 ml of diluted solutions were added to 15 ml of known concentration of caffeine solution).

Prior to applying the perturbation, the electrodes were kept in the solution for five minutes. A sinusoidal a.c perturbation voltage with r.m.s value of 10 mV was applied and the frequency was varied from 0.1 kHz to 20 kHz. The temperature of the solution was maintained at 296 ± 2 K. Each measurement was repeated thrice with 3 different samples of same batch and the standard deviation was calculated from the average of these three values. The EIS data were analyzed using NOVA software. To correlate the chemical kinetics with electrical behavior, an electrical equivalent circuit was modeled [27,28,29,30]. In particular, the Solution resistance (R_s), Charge Transfer Resistance (R_{ct}), Helmholtz double layer capacitance (C_{dl}), and diffusion double layer capacitance (C_{di}) were extracted from modeled circuits [31,32,33]. It is to be mentioned here that in order to deal with the non-linearity and inhomogeneity at the solution electrode interfacial surface, a constant phase element (CPE) was introduced in diffusion double layer capacitance [34,35,36,37]. The inhomogeneities of the diffusion layer is determined from the deviation of the exponent from the ideal values [38,39]. We found that the inclusion of CPE improves the quality of fitting and all the phenomenon is explained in the result and discussion section.

3. RESULTS AND DISCUSSION

3.1. Measurements of overall impedance

Electrochemical impedance spectroscopy reflects the impedance change due to chemical and electrochemical processes taking place at the electrode surface [40]. The results of an impedance measurement are usually represented by using Bode (modulus of Z vs. frequency) and Nyquist (real Z vs. Imaginary Z) plots for all applied frequencies [40]. In the following section standard curve is obtained by using Bode and Nyquist plots from a series of known concentrations of pure caffeine. Slopes of the calibrated curvatures and fitted parameters are then used to determine the concentration of unknown samples with variable caffeine concentrations. During calibration, caffeine concentrations were varied from 100 mM to $450 \mu\text{M}$. The Bode plots were recorded with different dilutions of pure caffeine solutions, (as shown in Figure 1 A - C). In the Bode plot a plateau region was observed at a frequency over 5 kHz. Below this frequency, the $|Z|$ value increased linearly with the decrease in frequency. The plateau region corresponds to resistive components at higher frequencies and the linear increase at lower frequencies indicates double layer capacitor formation at the electrode-electrolyte interface[41].

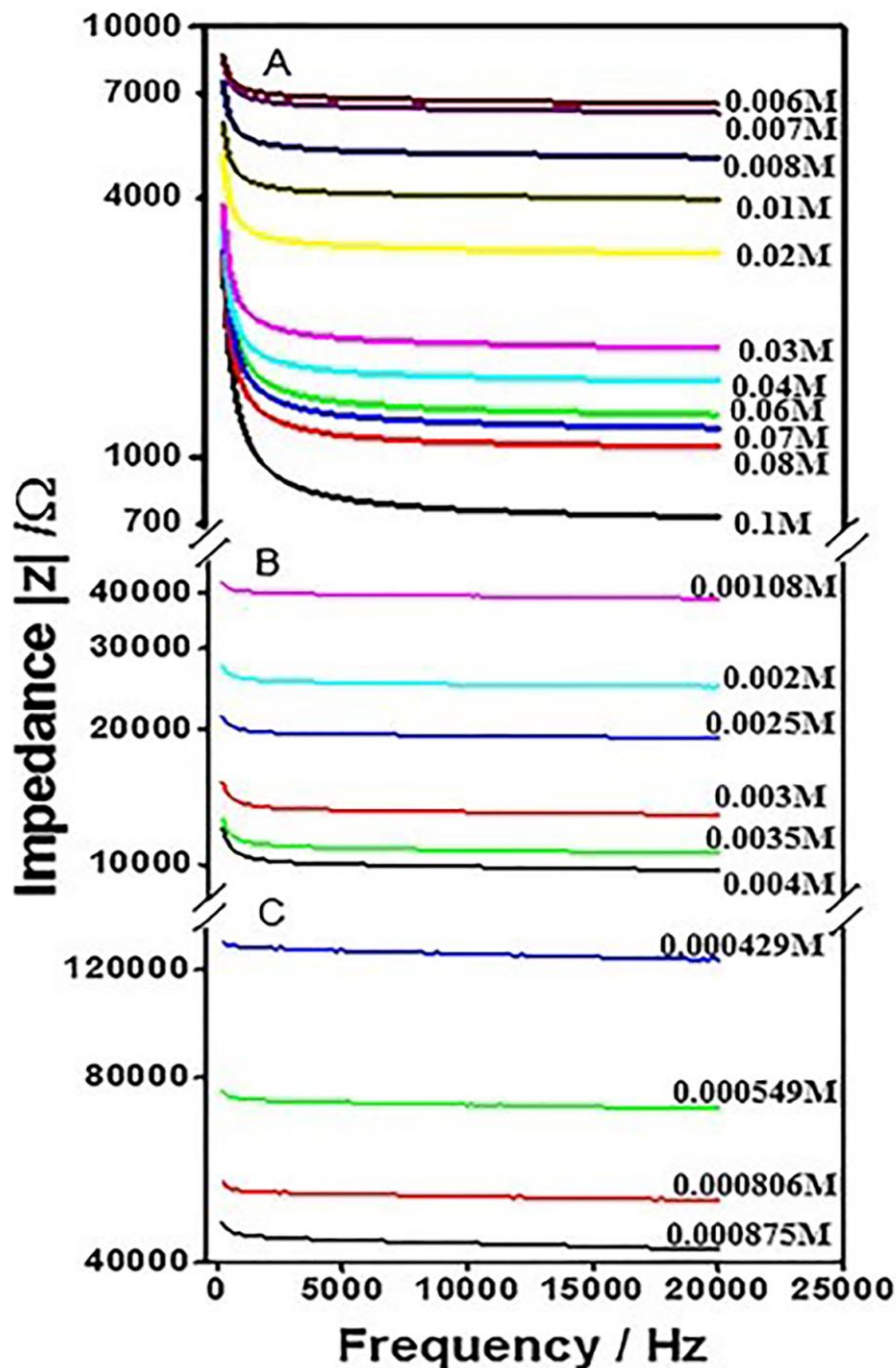


Figure 1. Bode plot (absolute impedance $|Z|$ vs. frequency) at various caffeine concentrations (429 μM to 100 mM) within the frequency range 100 Hz to 20 kHz. A. Bode plot at higher caffeine concentration range (0.1 M to 6 mM) B. Bode plot at caffeine concentration range 4 mM to 1.08 mM C. Bode plot at a low caffeine concentration (0.875 mM to 0.429 mM). A two electrode set up comprising of a platinum disc and a platinum wire was used. The solution temperature was maintained at 296 ± 2 K throughout the experiment.

In order to plot a calibration curve ($|Z|$ vs. caffeine concentrations), a fixed frequency was considered (~ 7 kHz) in the saturation region. The impedance measurement at the fixed frequency is an alternative technique to estimate analytes in electrochemical solution. It is to be mentioned that,

negate water's contribution in the impedance measurement of the solutions, all the measured impedance data were subtracted from the pure water impedance value. The change in impedance ($\Delta|Z| = |Z|_{\text{Water}} - |Z|_{\text{Caffeine}}$) was then plotted in Figure 2 as a function of caffeine concentration.

Mainly, two regions were observed with two different slopes. In the higher concentration region (>0.04 M) the slope was $5.5 \text{ k}\Omega \text{ M}^{-1}$ as compared to $69.3 \text{ k}\Omega \text{ M}^{-1}$ at a lower concentration region (<0.035 M), indicating greater sensitivity at lower concentrations. This is due to the fact that, at higher concentrations greater amount of caffeine molecules are attached at the interface and thus saturation occurred in the system, resulting in lesser change in the impedance value [41]. In the following section impedance spectra is further analyzed by using Nyquist plots in various concentrations of caffeine solution.

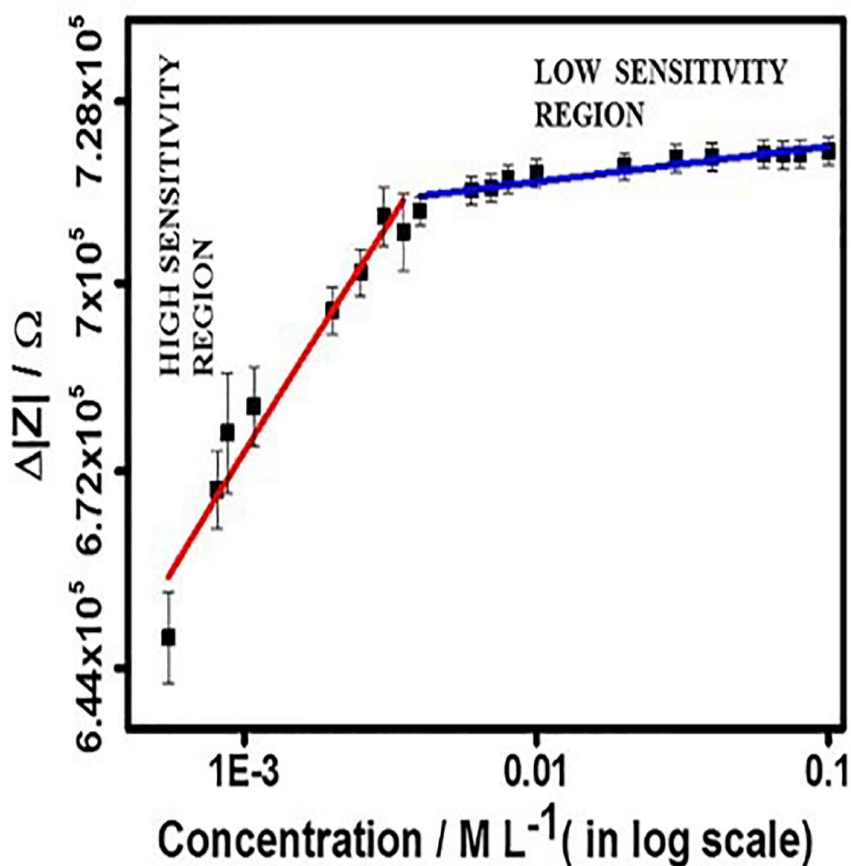


Figure 2. Calibration curve of variation in change of impedance ($\Delta|Z|$) of aqueous caffeine solution with caffeine concentrations, at a fixed frequency (7045 Hz). Here the dotted points represent the experimental impedance and the solid lines (blue and red) represent the linear fitting. Two distinct regions with different slopes indicate different sensitivities of the sensor.

3.2. Electrochemical circuit analysis

An equivalent electrical circuit was modeled for this electrochemical system by taking into account, all the circuit components (as explained earlier) that are present in the electrode-solution assembly and is shown in Figure 3 and Figure 4.

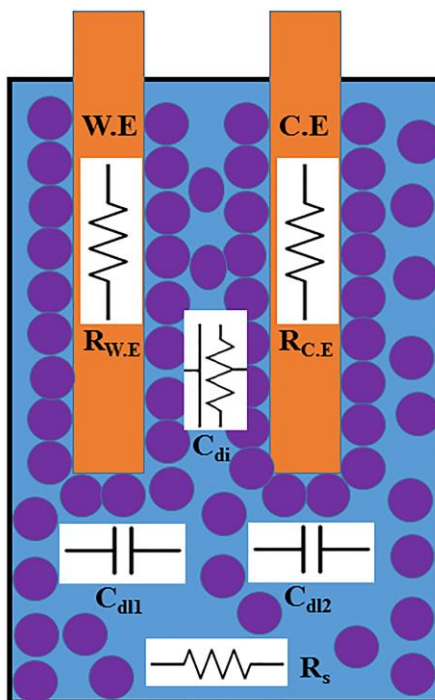


Figure 3. Schematic representation of electrode assembly with aqueous caffeine solution with different circuit parameters used for electrochemical modeling. A two electrode set up comprising of a platinum disc and a platinum wire were used as working and counter electrode respectively. Capacitances were formed at electrode-caffeine interfaces. The solution resistance generated for bulk caffeine solution. A diffusion capacitance was also formed in between the electrodes.

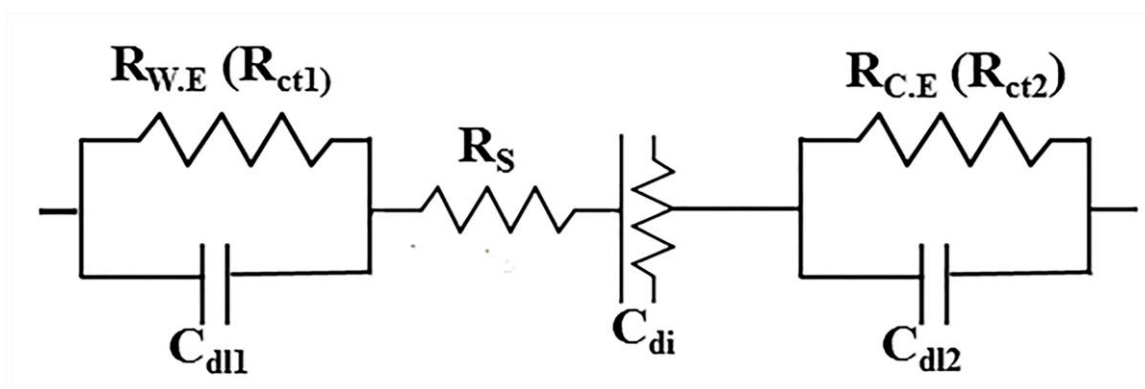


Figure 4. Equivalent circuit for the electrochemical cell using two electrodes and caffeine solution. Both electrodes consist of a parallel circuit with a double layer capacitance (C_{dl}) and a charge transfer resistance (R_{ct}). Solution resistance (R_s) and the constant phase element governed diffusion capacitance (C_{di}) are in series with the electrode impedances.

The circuit components are explained as: solution resistance (R_s) due to the potential drop in the bulk solution. Moreover, the application of electric field would generate two processes (charge transfer and electrical double layer formation) at the electrode- solution interface. The charge transfer (electron transfer) would be accompanied by the charge transfer resistance (R_{ct}) [42,43]. The double

layer capacitance (C_{dl}) arises due to strong coulombic interaction between the caffeine molecules and the electrodes, resulting in the formation of inner and outer Helmholtz layer (Stern layer) [44]. These two circuit components are parallel to each other. Just away from the interface, there are two opposing forces acting on caffeine molecules: i) attraction due to coulomb interaction, ii) Brownian motion due to thermal agitation. The resulting forces would attribute in the formation of a diffuse layer [41,45].

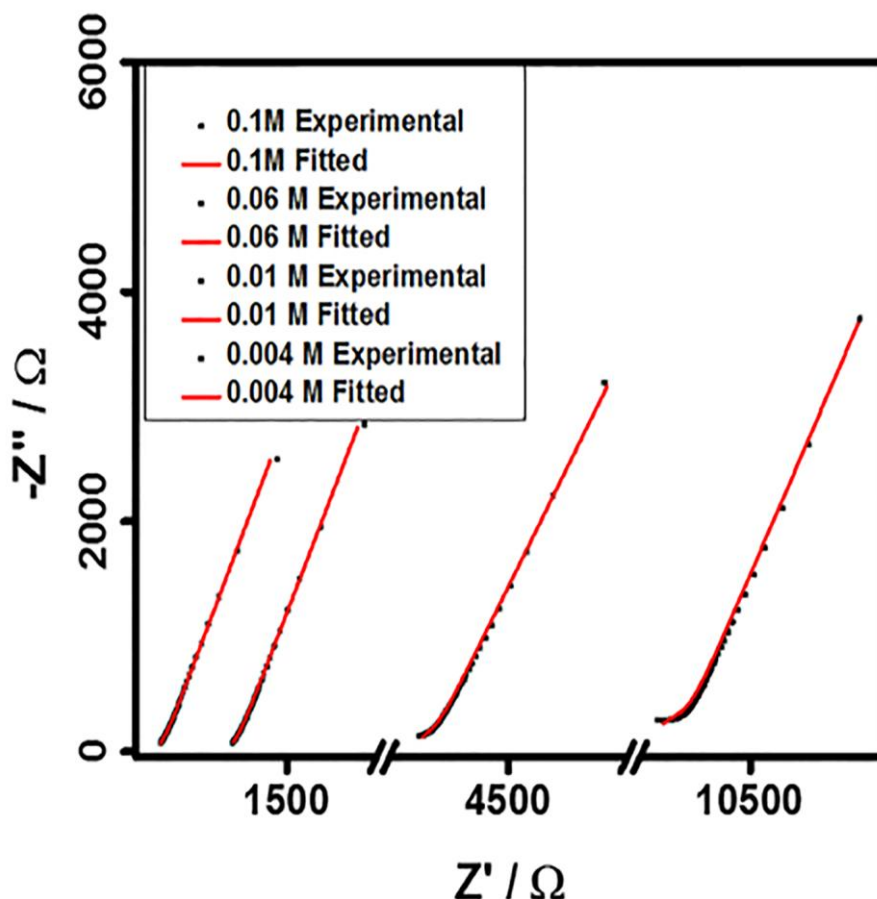


Figure 5. Nyquist plots (real impedance vs. imaginary impedance) of caffeine solution and the fitted impedance curves at four caffeine concentrations, within frequency range 100 Hz to 20 KHz. Dotted black points represent the experimental data and solid red lines represent the fitted spectrum of equivalent circuit. We applied an a.c perturbation voltage with r.m.s value 10 mV between disc and platinum wire electrodes.

The diffused layer is modeled as a C.P.E where both the resistive and capacitive behavior are included. The variation in potential and the non-linearity in the caffeine solution leads us to incorporate C.P.E in the model circuit, which allows us to estimate diffusion capacitance (C_{dl}) [39,46]. The solution resistance and the diffusion capacitance are in series with the parallel combinations at both sides making a complete electrical equivalent circuit (Figure 4). The similar type of equivalent circuit was also explored in impedance based Glucose sensors [28,41,47]. The impedances of the above mentioned circuit elements is mentioned in table 1.

Table 1. The impedance values of the different active and passive circuit elements (solution resistance, charge transfer resistance, double layer capacitance and diffusion capacitance) used in modeling the sensor

CIRCUIT ELEMENT	IMPEDANCE VALUE	
Solution resistance (R_s)	$Z=R$	R: Resistance
Charge transfer resistance (R_{ct})	$Z=R$	
Double layer capacitance (C_{dl})	$Z=1/j\omega C$	C: Capacitance $j=\sqrt{-1}$ ω : Frequency
Diffusion capacitance (C_{di})	$Z=Y_0 (j\omega)^{-\alpha}$ Where $Y_0 =1/C$ for $\alpha =1$ and for $Y_0=R$ for $\alpha =0$	

Nyquist plots were also recorded at four pure caffeine solutions are shown in Figure 5. The impedance data were fitted by using NOVA software [48,49]. Our equivalent circuit model (solid lines) as proposed in the previous section nicely matches with the experimental curve (dotted points). The nature of the Nyquist plots clearly suggests that the charge transfer at the interface is minimal and the diffusive mass transfer phenomena is dominant for all caffeine concentrations [28]. The residual X^2 value was <0.001 for all the fitting curves, indicating that the equivalent circuit model is coinciding with the experimental data very closely. All the equivalent circuit parameters are given in Table 2. These data suggest that the value of the solution resistance (R_s , in column 2) is increasing with the decrease in caffeine concentration. This is due to the fact that pure water has higher resistivity and with the introduction of more solutes (caffeine) there is an increase in conductivity.

The second important parameter is the exponent (n) in the C.P.E (Column 5 of II). The exponent indicates the capacitive or resistive nature of the system and the value of the exponent varies in between 0-1. The lower limit suggests that the system is purely resistive and the upper value shows complete capacitive nature. From the available data it is quite evident that with the increase in solutes (caffeine) the capacitive nature would also increase [50]. The exponent of the diffuse layer capacitance was thus plotted as a function of caffeine concentration and the plot showed a linear increase in the exponent value with the increase of caffeine concentration. The Table also showed that the charge transfer resistance (R_{ct}) at the solution-electrode interface decreases with the increase in caffeine concentration.

Table 2. Values of different circuit elements modeled using equivalent electrochemical circuit (Figure 4) and the residual X^2 values for each fitting. Analysis was carried out using the platinum disc and platinum wire electrodes. The obtained parameters were derived after equivalent circuit Fitting.

CONCEN TRATIO N (M)	R_s in k Ω	R_{ct1} in Ω	C_{dl1} in nano Farad	Y_0 in nmho & exponent of C.P.E	R_{ct2} in Ω	C_{dl2} in nano Farad	X^2
0.1	0.704	12.3	1190	864; 0.85	12.3	1190	0.00084
0.08	1.04	14.8	997	869; 0.84	16	2950	0.00039
0.07	1.23	27.2	528	802; 0.83	25.2	2220	0.00041
0.06	1.15	14.9	1140	789; 0.73	14.9	677	0.00012
0.04	1.49	15.2	3090	863; 0.83	25.2	602	0.00089
0.03	1.78	20.6	3310	856; 0.82	39.6	439	0.0015
0.02	2.96	28.2	628	886; 0.80	28.3	624	0.00178
0.01	3.95	38	335	906; 0.79	38	335	0.00128
0.008	4.94	45.9	279	862; 0.78	45.9	279	0.00165
0.007	6.25	75.2	144	995; 0.76	75.2	144	0.0011
0.006	6.57	73.8	154	1060; 0.76	73.7	154	0.00149
0.004	9.65	118	85.9	1010; 0.75	118	85.9	0.00145
0.0035	12.7	193	38.8	1120; 0.74	193	38.8	0.00059
0.003	10.5	139	67.3	1110; 0.76	139	67.3	0.0011
0.00025	18.3	500	9.77	1150; 0.74	500	9.77	0.00017
0.002	23.3	850	4.95	1320; 0.70	850	4.95	0.00034
0.00108	35.2	2090	1.87	1360; 0.69	2090	1.87	0.00024
0.000875	39.3	1960	2.95	1720; 0.65	1960	2.95	0.0011
0.000805	44.2	7220	0.459	1230; 0.70	177	132	0.00024
0.000549	49.6	22900	0.0947	1140; 0.69	440	58.5	0.00012
Water	131	593000	0.707	0	591000	0.0103	0.0075

On the other hand, the double layer capacitance (C_{dl}) increases with the increase of caffeine concentration. The parametric values of R_{ct} and C_{dl} nicely match with the experimental curve in Nyquist plot.

The values of $1/R_s$ were plotted against various caffeine concentrations (as shown in Figure 6). The plot shows a linear response with a correlation coefficient of 0.9946 indicating a perfect linear response of the sensor. The exponent of the diffuse layer capacitance (n) was also plotted with

concentration (as shown in Figure 7). The plot showed a linear increase in the exponent value with the increase in caffeine concentration.

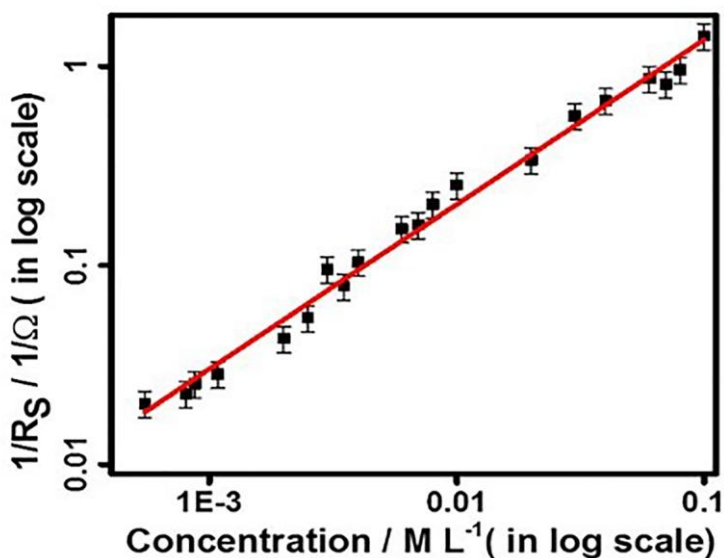


Figure 6. Calibration curve of aqueous caffeine solution (inverse of solution resistance (R_s) vs. caffeine concentrations) obtained from Nyquist data (shown in table 2). Black points represent the experimental values and the solid red line represents the linear fitting. The error bar is calculated from standard deviation.

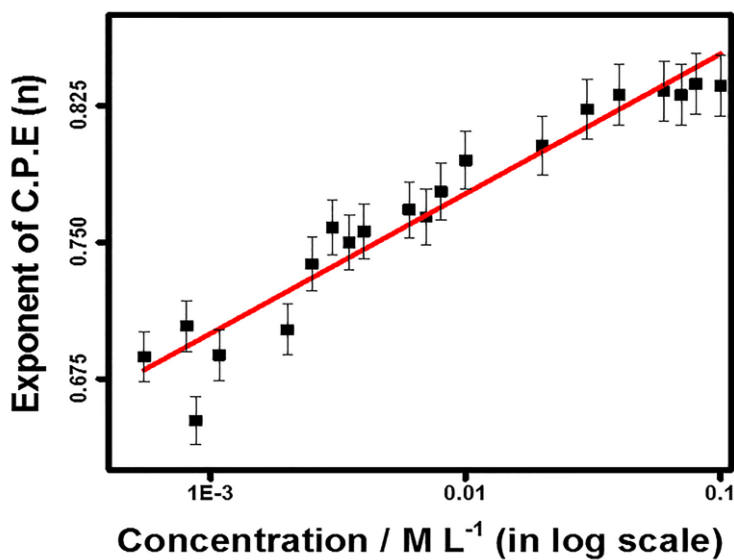


Figure 7. Calibration curve of aqueous caffeine solution (exponent of C.P.E (n) vs. caffeine concentrations) obtained from Nyquist data (shown in table 2). Black points represent the experimental values and the solid red line represents the linear fitting. The error bar is calculated from standard deviation.

Above results and discussion clearly indicate that the experimental value of $|Z|$, and all fitted parameters can be utilized to detect caffeine in real samples such as food and beverages. In the current study, $\Delta|Z|$, $1/R_s$ and n values are compared with the caffeine concentration of cola beverages.

3.3. Analysis of caffeine in cola beverages

Three cola beverages were bought from the market in bottles. Each sample was kept in a glass beaker and ultrasonicated for half an hour to remove the dissolved carbon dioxide. Next, all the samples were diluted individually 10-15 times by using DI water. These samples were further mixed with known concentrations of caffeine solutions and the impedance measurements were carried out. It is important to mention that to minimize the matrix effect of the cola samples [51] and to measure the impedance values in the higher sensitive region of the calibration curve the caffeine solutions were diluted by using DI water. Furthermore, in order to study the matrix effect qualitatively standard pure caffeine solution was added to the diluted cola beverage samples [19]. Again, Bode plots were analyzed to obtain $|Z|$ values and Nyquist plots were fitted with the same equivalent circuit to obtain the values of R_s , R_{ct} , n , and C_{dl} .

From the datasheets of the cola beverage manufacturers and from the literature the amount of caffeine in those beverages was recorded. The amount of caffeine contents in as bought CB1, CB2 and CB3 are 105.67 mg L^{-1} , 152.54 mg L^{-1} , and 96.05 mg L^{-1} respectively. It is important to mention here that for each samples the measurements were carried out by using 30 ml of solution, containing 15 ml of diluted cola beverage and 15 ml of known pure caffeine solution. Cola beverages with various molar concentrations of caffeine were prepared to compare their performance with known caffeine solutions.

At first, the values of the impedance corresponding to this molar concentration were obtained from the calibration curve (Figure2). Table 3 represents the experimental ($\Delta|Z|$) values of the three beverages and the corresponding $\Delta|Z|$ values obtained from the calibration curve of Figure 2. It is obvious from the Table 3 that irrespective of cola beverages the difference in impedance ($\Delta|Z|$) values increases with the increase of molar concentration of the caffeine. The trends of variation also satisfy the difference in impedance ($\Delta|Z|$) obtained from calibration data (column 4 of Table 3).

In this work, an attempt was also made to evaluate recovery of the caffeine in cola beverages.

We propose that the percentage recovery (RP) could be defined as: $RP = (\Delta|Z|_{Exp} / \Delta|Z|_{Cal}) * 100\%$, (Table 3). Similar percentage recovery of chemical species is reported elsewhere [19,52]. The percentage recovery of caffeine in all the samples is also noted in Table 3. The percentage recovery was varying from $((102\%-104\%) \pm (1-2\%))$. Cola beverage solutions not only possess caffeine, but also have different sugars, carbohydrate, fat and other components. So the impedance of these components may also add up to the desired value and hence the recovery was greater than 100 %. The experiments were followed for each cola beverage sample spiked with different pure caffeine concentration and it has been found that the trend remained same in all the cases which confirm the presence of those elements.

Table 3. Experimental and calibrated values of modulus of difference in impedance ($\Delta|Z|$) for 3 different Cola beverages at two different dilutions (C/10 and C/15) spiked with caffeine solution of two different concentrations and the percentage recoveries of caffeine in cola beverages diluted by 1/10 and 1/15 from initial concentration. The measurements were taken using platinum disc and platinum wire electrodes. The experimental values were measured from the Bode plot and the calibrated impedance was obtained from calibration curve.

Pure Caffeine con. mM L ⁻¹	Sample	Sample Concentration mM L ⁻¹	Experimental Impedance ($\Delta Z_{Exp} $) in k Ω	Calibrated Impedance ($\Delta Z_{Cal} $) in k Ω	Percentage Recovery RP= ($\Delta Z_{Exp} /\Delta Z_{Cal} $) × 100 %
1	CB1 C/10	1.054	701.2	676.5	103.65%
	CB2 C/10	1.080	701.8	677.3	103.62%
	CB3 C/10	1.049	699.8	676.3	103.47%
	CB1 C/15	1.037	696.5	676.1	103.02%
	CB2 C/15	1.052	697.2	676.3	103.01%
	CB3 C/15	1.032	695.3	673.4	103.25%
0.8	CB1 C/10	0.085	701.5	671.3	104.50%
	CB2 C/10	0.088	701.7	671.7	104.47%
	CB3C/10	0.085	698.8	670.2	104.27%
	CB1 C/15	0.084	694.1	669.5	103.67%
	CB2 C/15	0.085	695.7	670.1	103.82%
	CB3 C/15	0.083	693.2	669.3	103.57%

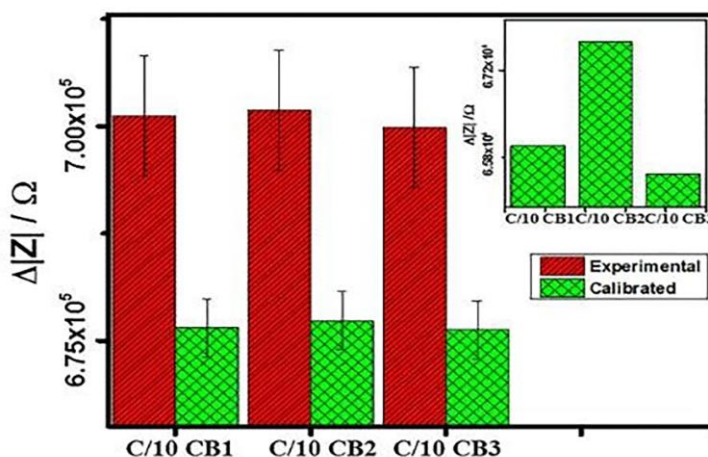


Figure 8. Bar diagram of difference in impedance ($\Delta|Z|$) of three cola beverages. Red dense cross lines represent the experimental obtained results and the green sparse line represents the values obtained from the calibration curve. Inset shows the magnified view of calibrated impedance for three different samples. The cola beverages were spiked with 0.001 M of pure caffeine. The measurements were taken using platinum disc and platinum wire electrodes. The experimental values were measured from the Bode plot and the calibrated impedance was obtained from calibration curve.

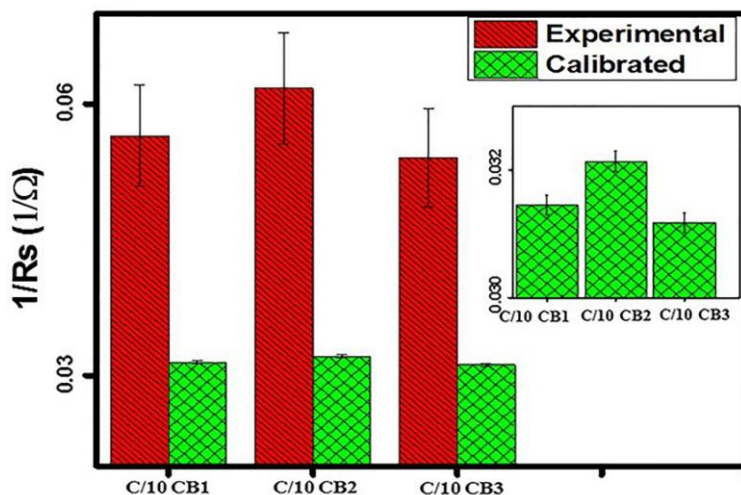


Figure 9. Bar Diagram of inverse solution resistance of three cola beverages spiked with 0.001 M pure caffeine solution. Red dense cross lines represent the experimentally obtained results and the green sparse line represents the values obtained from the calibration curve. Inset shows the magnified view of calibrated inverse of solution resistance for three beverages. The measurements were taken using platinum disc and platinum wire electrodes. The experimental values were measured from the Bode plot and the calibrated impedance was obtained from calibration curve.

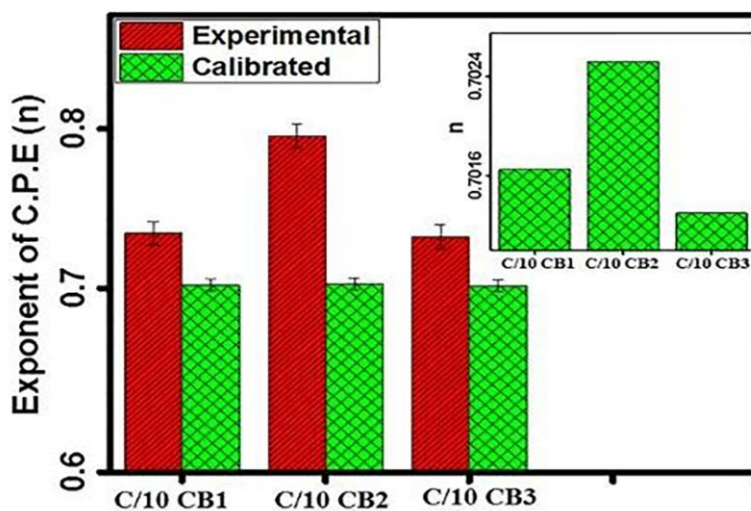


Figure 10. Bar diagram of exponent of C.P.E (n) for three cola beverages. Red dense cross lines represent the experimental obtained results and the Green sparse line represents the values obtained from the calibration curve. Inset shows the magnified view of calibrated exponent for three beverages. The cola beverages were spiked with 0.001 M of pure caffeine. The measurements were taken using platinum disc and platinum wire electrodes. The experimental values were measured from the Bode plot and the calibrated impedance was obtained from calibration curve.

Figure 8 gives the representation of experimental and calibrated difference in impedance values ($\Delta|Z|$) for three different cola beverages. (Inset represents the calibrated impedance of the beverages). From the literature we found that the caffeine concentration in sample CB2 was highest and the same for CB3 was lowest (Caffeine level in, $CB2 > CB1 > CB3$). From our calibrated curve, it was also observed that $\Delta|Z|$ increases upon the addition of caffeine in the standard solution. The measurements depicted in the Figure 9 also showed the similar trend. (i.e. $Z_{CB2} > Z_{CB1} > Z_{CB3}$). Further the equivalent circuit parameters of these samples were also analyzed and plotted (as shown in Figure 9. and Figure 10). It represents the experimental and calibrated values obtained from the calibration curves (Figure 6 and Figure 7) for the inverse solution resistance ($1/R_s$) and exponent of the constant phase element (n) respectively. For every sample red bar represent the signal obtained from the measurements of caffeine in the real samples and the value obtained from the calibration standard curve is shown in the green bar. The data obtained from the circuit fitting of the caffeine solutions showed solution resistance was inversely proportional to caffeine concentration and constant phase element (n) was directly proportional the caffeine concentration. A clear trend in the variation of difference in impedance, n and $1/R_s$ with caffeine concentration was observed in both experimental and calibrated histograms. The experimental plots in Figure 8, Figure 9 and Figure 10 are in agreement with the caffeine levels mentioned in all three samples. The above results are promising and clearly suggest that understanding difference in impedance and other electrical circuit elements will be very useful for sensing the caffeine level in real samples.

Table 4 represents a comparison table among different conventional techniques used for caffeine detection. Caffeine in pure form or caffeine in commercial beverages are usually detected using these techniques. In our present work, we show that we can detect caffeine in the cola beverages with caffeine content $\sim 96 \text{ mg L}^{-1}$ using electrochemical impedance spectroscopy, which is comparable to the other available detection techniques. However, further surface modifications and functionalization of electrode surface will enhance the sensitivity and limit of detection of the sensor.

Table 4. A comparison table of available conventional techniques for the detection of pure caffeine and caffeine content in commercial beverages. The detected caffeine content in the present work is also shown.

Technique	Type of Caffeine	Lowest detectable limit	Detected caffeine content	Reference
Liquid chromatography and atmospheric pressure chemical ionization mass spectrometry	Pure	4 ng lit-1	_____	[16]

High-performance thin-layer chromatography (HPTLC) with mass spectrometry (MS)	Real Samples (energy drinks (E.D) pharmaceutical tablets)	_____	320 mg lit-1 for E.D	[17]
Fourier transform infrared spectrometry	Black Tea Leaf	35 ng lit-1	_____	[18]
Differential Pulse Voltammetry	Commercial Beverages (Coffee, tea, cola beverages, Energy Drinks)	_____ -	117 mg lit -1 for cola beverages	[19]
cyclic voltammetry (CV) and adsorptive stripping differential pulse voltammetry (AdSDPV)	Pure	8.3X10-8M	_____	[21]
Electrochemical Impedance spectroscopy	Commercial cola beverages	_____	96 mg L ⁻¹	Present work

4. CONCLUSIONS

In this work, impedance change due to molecular interaction at the electrode-solution interface was investigated for the estimation of caffeine in standards and real samples. In order to understand the fundamental characteristics of the interaction, electrochemical impedance spectra from the sensor were modeled by using a developed equivalent electrical circuit model. From the overall impedance data at a single frequency, it was found that there is a rapid increment of sensitivity in the lower caffeine concentration region than that in the higher concentration region. In addition, inverse of solution resistance and constant phase element values were also observed varying linearly with the caffeine concentrations. Finally, we have demonstrated that above standard curves were very useful for a comparative study of caffeine levels in real cola beverages. This work would certainly contribute to a better understanding of the interfacial phenomena occurred at caffeine modified electrode and in future to develop EIS based caffeine sensors.

ACKNOWLEDGEMENT

Mr. Gourav Bhattacharya is indebted to Shiv Nadar University for providing PhD scholarship.

References

1. B. A. Weinberg and B. K. Bealer, *The world of caffeine: the science and culture of the world's most popular drug*, Psychology Press, (2001).
2. J. Barone and H. Roberts, in *Caffeine*, Springer, (1984).
3. A. Nehlig, J.-L. Daval and G. Debry, *Brain Research Reviews*, 17 (1992) 139.
4. G. Fisone, A. Borgkvist and A. Usiello, *Cellular and Molecular Life Sciences CMLS*, 61 857.
5. M. A. Heckman, J. Weil, D. Mejia and E. Gonzalez, *Journal of Food Science*, 75 (2010) R77.
6. P. Esquivel and V. M. Jiménez, *Food Research International*, 46 (2012) 488.
7. R. B. Lipton, W. F. Stewart, R. E. Ryan, J. Saper, S. Silberstein and F. Sheftell, *Archives of neurology*, 55 (1998) 210.
8. D. E. Grobbee, E. B. Rimm, E. Giovannucci, G. Colditz, M. Stampfer and W. Willett, *New England Journal of Medicine*, 323 (1990) 026.
9. B.-B. S. Zhou, P. Chaturvedi, K. Spring, S. P. Scott, R. A. Johanson, R. Mishra, M. R. Mattern, J. D. Winkler and K. K. Khanna, *Journal of Biological Chemistry*, 275 (2000) 10342.
10. M. Giannelli, P. Doyle, E. Roman, M. Pelerin and C. Hermon, *Paediatric and perinatal epidemiology*, 17 (2003)316.
11. A. Nehlig, *Neuroscience & Biobehavioral Reviews*, 23 (1999) 563.
12. P. Stephenson, *Journal of the American Dietetic Association*, 71 (1977) 240.
13. G. A. Tanner and J. A. Tanner, *American journal of kidney diseases*, 38 (2001) 1089.
14. T. Roehrs and T. Roth, *Sleep medicine reviews*, 12 (2008) 153.
15. C. Huck, W. Guggenbichler and G. Bonn, *Analytica chimica acta*, 538 (2005) 195.
16. P. R. Gardinali and X. Zhao, *Environment International*, 28 (2002) 521.
17. H. Luftmann, M. Aranda and G. E. Morlock, *Rapid Communications in Mass Spectrometry*, 21 (2007) 3772.
18. N. M. Najafi, A. S. Hamid and R. K. Afshin, *Microchemical Journal*, 75 (2003) 151.
19. W. Y. Khoo, M. Pumera and A. Bonanni, *Analytica chimica acta*, 804 (2013) 92.
20. H. Cai, Y. Wang, P. He and Y. Fang, *Analytica chimica acta*, 469 (2002) 165.
21. B. J. Sanghavi and A. K. Srivastava, *Electrochimica Acta*, 55 (2010) 8638.
22. P. Luo, F. Zhang and R. P. Baldwin, *Analytica chimica acta*, 244 (1991) 169.
23. C. Ruan, L. Yang and Y. Li, *Analytical Chemistry*, 74 (2002) 4814.
24. Y. Xu, Y. Jiang, H. Cai, P.-G. He and Y.-Z. Fang, *Analytica chimica acta*, 516 (2004) 19.
25. J. Luo, S. Jiang, H. Zhang, J. Jiang and X. Liu, *Analytica chimica acta*, 709 (2012) 47.
26. S. Gernet, M. Koudelka and N. De Rooij, *Sensors and Actuators*, 18 (1989) 59.
27. J. Suehiro, G. Zhou and M. Hara, *Journal of Physics D: Applied Physics*, 36 (2003) L109.
28. R. K. Shervedani, A. H. Mehrjardi and N. Zamiri, *Bioelectrochemistry*, 69 (2006) 201.
29. H. Chen, C. K. Heng, P. D. Puiu, X. D. Zhou, A. C. Lee, T. M. Lim and S. N. Tan, *Analytica chimica acta*, 554 (2005) 52.
30. Q. Xie, J. Wang, A. Zhou, Y. Zhang, H. Liu, Z. Xu, Y. Yuan, M. Deng and S. Yao, *Analytical chemistry*, 71 (1999) 4649.
31. J. R. Scully, D. C. Silverman and M. W. Kendig, *Electrochemical impedance: analysis and interpretation*, ASTM International, (1993).
32. J. Chmiola, C. Largeot, P. L. Taberna, P. Simon and Y. Gogotsi, *Angewandte Chemie*, 120 (2008) 3440.
33. R. De Levie, *Electrochimica Acta*, 8 (1963) 751.

34. G. Brug, A. Van Den Eeden, M. Sluyters-Rehbach and J. Sluyters, *Journal of electroanalytical chemistry and interfacial electrochemistry*, 176 (1984) 275.
35. P. Zoltowski, *Journal of Electroanalytical Chemistry*, 443 (1998) 149.
36. R. K. Shervedani and S. A. Mozaffari, *Analytica chimica acta*, 562 (2006) 223.
37. S. E. Creager and T. T. Wooster, *Analytical Chemistry*, 70 (1998) 4257.
38. B. Hirschorn, M. E. Orazem, B. Tribollet, V. Vivier, I. Frateur and M. Musiani, *Journal of The Electrochemical Society*, 157 (2010) C452.
39. S. Roy, N. Soin, R. Bajpai, D. Misra, J. A. McLaughlin and S. S. Roy, *Journal of Materials Chemistry*, 21 (2011) 14725.
40. J. R. Macdonald and E. Barsoukov, *History*, 1 (2005) 8.
41. C. Tlili, K. Reybier, A. Gélœn, L. Ponsonnet, C. Martelet, H. B. Ouada, M. Lagarde and N. Jaffrezic-Renault, *Analytical chemistry*, 75 (2003) 3340.
42. J. Bobacka, *Analytical chemistry*, 71 (1999) 4932.
43. M. E. Ghica and C. M. Brett, *Analytica chimica acta*, 53 (2005) 145.
44. N. A. Chaniotakis, Y. Alifragis, G. Konstantinidis and A. Georgakilas, *Analytical chemistry*, 76 5552.
45. J. De Wit, W. Van Riemsdijk, M. Nederlof, D. Kinniburgh and L. Koopal, *Analytica chimica acta*, 232 (1990) 189.
46. Z. Chen, J. Jiang, G. Shen and R. Yu, *Analytica chimica acta*, 553 (2005) 190.
47. F. Lisdat and D. Schäfer, *Analytical and bioanalytical chemistry*, 391 (2008) 1555.
48. L. Lu, G. Chee, K. Yamada and S. Jun, *Biosensors and Bioelectronics*, 42 (2013) 492.
49. J. Casanova-Moreno and D. Bizzotto, *Analytical chemistry* (2015).
50. C. Hsu and F. Mansfeld, *Corrosion*, 57 (2001) 747.
51. H. Stahnke, S. Kittlaus, G. n. Kempe and L. Alder, *Analytical chemistry*, 84 (2012) 1474.
52. J.-Y. Sun, K.-J. Huang, S.-Y. Wei, Z.-W. Wu and F.-P. Ren, *Colloids and Surfaces B: Biointerfaces*, 84 (2011) 421.